



**HAL**  
open science

## Excitation into high-lying states in Li 3+ -H collisions

Aicha Ibaaz, Rosa Esteban Hernandez, Alain Dubois, Nicolas Sisourat

► **To cite this version:**

Aicha Ibaaz, Rosa Esteban Hernandez, Alain Dubois, Nicolas Sisourat. Excitation into high-lying states in Li 3+ -H collisions. *Journal of Physics B: Atomic, Molecular and Optical Physics*, 2016, 49 (8), pp.085202 10.1088/0953-4075/49/8/085202 . hal-01314829

**HAL Id: hal-01314829**

**<https://hal.sorbonne-universite.fr/hal-01314829>**

Submitted on 12 May 2016

**HAL** is a multi-disciplinary open access archive for the deposit and dissemination of scientific research documents, whether they are published or not. The documents may come from teaching and research institutions in France or abroad, or from public or private research centers.

L'archive ouverte pluridisciplinaire **HAL**, est destinée au dépôt et à la diffusion de documents scientifiques de niveau recherche, publiés ou non, émanant des établissements d'enseignement et de recherche français ou étrangers, des laboratoires publics ou privés.

# Excitation into high-lying states in $\text{Li}^{3+}$ -H collisions.

Aicha Ibaaz,<sup>1</sup> Rosa Esteban Hernandez,<sup>1</sup> Alain Dubois,<sup>1</sup> and Nicolas Sisourat<sup>1</sup>

<sup>1</sup>*Sorbonne Universités, UPMC Univ Paris 06, CNRS,  
Laboratoire de Chimie Physique Matière et Rayonnement, F-75005, Paris, France*

\*

(Dated: May 11, 2016)

## Abstract

We have studied the excitation of atomic hydrogen by fully-stripped lithium ion impact in the intermediate energy range using a new and efficient implementation of the two-center atomic orbital approach with Gaussian-type orbitals. Partial and state-selective cross sections have been obtained for excitation up to H(6h). A careful investigation of the convergence of the results with respect to the basis set has been performed which allows to estimate the accuracy of the cross sections. Furthermore, our calculations provide an explanation to the discrepancies between previous calculations on this collision system.

---

\* Nicolas.Sisourat@upmc.fr

## I. INTRODUCTION

Cross sections for electron capture, excitation and ionization processes occurring in the course of collisions between highly-charged ions and hydrogen atoms in the keV energy range are required as input data for the modeling and diagnosis of plasma through charge exchange recombination (CXR) [1] and beam emission (BE) [2, 3] spectroscopies. Collisions between fully-stripped ions and hydrogen atoms represent the simplest collisional systems and have been extensively investigated (see for example [4–13]). Cross sections for the dominant channels are known fairly accurately in a wide range of impact energy. However weaker channels which are important to model CXR and BE spectroscopies, like for example excitation into high-lying states ( $n \geq 3$ ), have been less considered.

In this context the collision between fully-stripped lithium ion and hydrogen atom in the keV energy range is of particular interest for fusion energy research. While this system has been extensively studied (see [14] for a recent review), cross sections for electron capture and excitation into high-lying states are still not known accurately. Recently, Suarez *et al.* [15] used a combination of semi-classical molecular and one-center atomic-orbital close-coupling approaches as well as a Classical Trajectory Monte Carlo model to propose  $n$ -resolved excitation cross sections into H( $n=2-6$ ) states for impact energy from 15 keV/u to 1000 keV/u. Lower impact energies down to 1 keV/u have also been considered by the authors. However, due to practical basis set limitations only excitation cross sections into H( $n=2-3$ ) states have been reported. Furthermore, Liu *et al.* [16] employed a two-center atomic-orbital close-coupling approach to compute the cross sections for electron excitation to  $n=2$  and  $n=3$  shells of H atom in the 1-100 keV/u energy range. For energy above 30 keV/u, their cross sections are larger than those of Suarez *et al.* [15]: for excitation towards H( $n=2$ ) the differences reach up to 15% while the cross sections for excitation into H( $n=3$ ) may differ by more than a factor of 2 at some energies. State-selective ( $n\ell$ -resolved) excitation cross sections, which are necessary for low-density plasma diagnosis for which  $\ell$ -statistical distribution cannot be assumed [3, 17–19], have been only reported up to H( $4f$ ) by Toshima *et al.* [20], Purkait [21] and Martin [12]. The latter considered impact energies above 75 keV/u only. Differences of more than a factor of 2 are also observed for excitation into the highest excited states considered. It is therefore clear that the uncertainties on the cross sections for excitation in this system and in this important energy range are too large for

an accurate simulation of CXR and BE spectroscopies.

Except for the work of Purkait [21], all published results have been obtained within the straight-line impact parameter approach [22] and a close-coupling method, either within one or two-center basis set expansion and with Gaussian or Slater type orbitals. The differences between the results thus lie only on the basis set used, i.e. in the description of the states and/or the number of channels included in the calculations. In the present work, we have computed the excitation cross sections up to  $H(n=6, \ell=5)$  states in the 1-100 keV/u energy range using a two-center atomic-orbital close-coupling approach and extensive basis sets. A careful study of the convergence of the results with respect to the basis sets has been performed. Our results allow to conclude on the differences observed between the two most recently calculated excitation cross sections to  $H(n=2)$  and  $H(n=3)$  and provides accurate cross sections for higher-lying excited states. Furthermore, we present  $n\ell$ -resolved excitation cross sections.

The outline of the article is the following: the impact parameter method and the implementation used in our work are detailed in the next section. In section III.A, the cross sections for excitation into  $H(n=2)$  and  $H(n=3)$  are presented and convergence with respect to the basis sets is discussed. The cross sections for excitation into  $H(n=4-6)$  states are examined in section III.B. In sections III.C, we report on the recommended  $n\ell$ -resolved excitation cross sections. The article ends with the conclusions of the work.

## II. METHODS

We used the well established impact parameter method [22] in which the nuclei follow classical trajectories while a quantum treatment describes the electronic dynamics. In the collision energy range considered here, the momentum transfer is small compared to the momentum of the collision partners so that straight-line trajectories can be assumed [22, 23]. The position vector of the projectile relative to the target is given by  $\vec{R}(t) = \vec{b} + \vec{v}t$  (see Fig.1) where  $\vec{b}$  and  $\vec{v}$  are the impact parameter and projectile velocity, respectively. The time-dependent Schrödinger equation for the electron reads

$$\left[ H - i \frac{\partial}{\partial t} \right] \Psi(\vec{r}, \vec{R}(t)) = 0 \quad (1)$$

with the electronic Hamiltonian

$$H = \left[ -\frac{1}{2}\nabla^2 + V_T(r) + V_P(|\vec{r} - \vec{R}(t)|) \right] \quad (2)$$

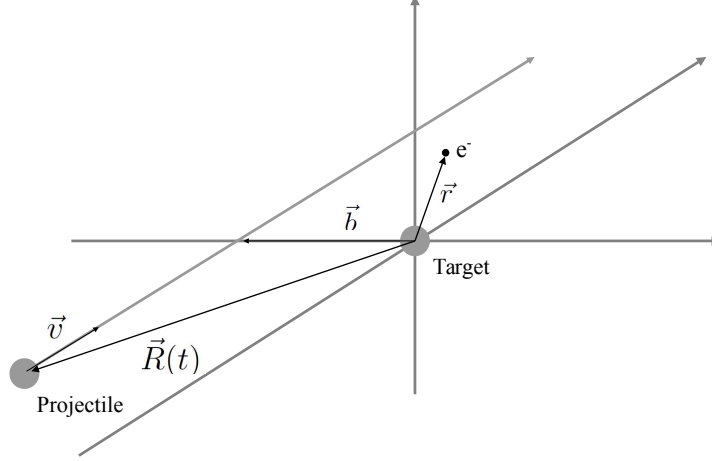


Figure 1. Collision geometry. The impact parameter  $\vec{b}$  and the projectile velocity  $\vec{v}$  define the collision plane. The position of the electron with respect to the target center is denoted  $\vec{r}$ .

where the potentials  $V_T(r)$  and  $V_P(|\vec{r} - \vec{R}(t)|)$  between the electron and the two nuclei are coulombic. The core-core potential between the bare ions only contributes through a global phase and is thus taken out. The Schrödinger equation is solved by expanding the wavefunction on a basis states of the isolated collision partners:

$$\Psi(\vec{r}, \vec{R}(t)) = \sum_i c_i^T(t) \Psi_i^T(\vec{r}) e^{-i\epsilon_i^T t} + \sum_j c_j^P(t) \Psi_j^P(\vec{r}) e^{-i\epsilon_j^P t} e^{i\vec{v}\cdot\vec{r} + i\frac{1}{2}v^2 t} \quad (3)$$

where  $\Psi_i^T$  and  $\Psi_j^P$  denote states where the electron is bounded to the target or to the projectile, respectively. The energy of the target and projectile states are labeled  $\epsilon_i^T$  and  $\epsilon_j^P$ , respectively. Note that the projectile-centered states contain the plane-wave electron translation factor (ETF),  $e^{i\vec{v}\cdot\vec{r} + i\frac{1}{2}v^2 t}$ , ensuring Galilean invariance of the results.

The insertion of Eq.(3) into Eq.(1) results in a system of first-order coupled differential equations for the time-dependent expansion coefficients  $c_i(t)$ , written in matrix form:

$$i\mathbf{S}(b, v, t) \frac{d}{dt} c = \mathbf{M}(b, v, t) c \quad (4)$$

where  $c$  is the column vector of the coefficients  $c_i$ ,  $\mathbf{S}$  and  $\mathbf{M}$  are respectively, the overlap and the coupling matrices. This equation is solved for a set of initial conditions using the Adams-Bashforth-Moulton predictor-corrector integrator. The transition probabilities for an impact parameter and projectile velocity are given by the coefficients  $c_i$  as following

$$P_f(b) = \lim_{t \rightarrow \infty} |c_f(b, t)|^2. \quad (5)$$

Cross section for a given electronic process leading to the transition to the final state  $f$  is calculated as

$$\sigma_f = 2\pi \int_0^{+\infty} b P_f(b) db. \quad (6)$$

In our implementation of the impact parameter method, we use linear combination of Cartesian Gaussian-type orbitals (GTO) to describe the target ( $\Psi_i^T(\vec{r})$ ) and projectile ( $\Psi_j^P(\vec{r})$ ) states:

$$\chi_k(\vec{r}) = N_k x^{u_k} y^{v_k} z^{w_k} e^{-\alpha_k r^2} \quad (7)$$

where  $N_k$  is a normalization factor and  $u_k$ ,  $v_k$  and  $w_k$  are integers. The exponents  $\alpha_k$  are chosen to provide even-tempered basis sets (see Supplementary data), ensuring thus an even coverage of the Hilbert space [24].

The computations of the overlap and coupling matrix elements required the evaluation of the following integrals:

$$S_{lmn} = \int d\vec{r} x^l y^m z^n e^{-\alpha r^2 + i\vec{v} \cdot \vec{r}} \quad (8)$$

and

$$V_{lmn} = \int d\vec{r} x^l y^m z^n e^{-\alpha r^2 + i\vec{v} \cdot \vec{r}} \frac{e^{-\beta(r-R_i)^2}}{|\vec{r} - \vec{R}_i|} \quad (9)$$

where  $R_i$  and  $\beta$  are chosen to describe the true potential or a model one. In the former case,  $\beta$  is set to zero and  $R_i$  is the position of a nuclei. In the present work, these integrals are evaluated according to recursion relations, which reduce significantly the cost of the matrix element computations, especially when high angular momentum orbitals are considered. The overlap integral  $S_{lmn}$  can be written as

$$S_{lmn} = \lim_{\vec{a} \rightarrow \vec{v}} (-i \frac{\partial}{\partial a_x})^l (-i \frac{\partial}{\partial a_y})^m (-i \frac{\partial}{\partial a_z})^n \left(\frac{\pi}{\alpha}\right)^{\frac{3}{2}} e^{-(v_x^2 + v_y^2 + v_z^2)/(4\alpha)}. \quad (10)$$

From this equation one can obtain the following recursion relation :

$$S_{lmn} = -\frac{(l-1)}{2\alpha} S_{(l-2)mn} - \frac{v_x}{2\alpha} S_{(l-1)mn} \quad (11)$$

Similarly, the potential integral can be written as

$$V_{lmn}^{(0)} = \lim_{\vec{a} \rightarrow \vec{v}} (-i \frac{\partial}{\partial a_x})^l (-i \frac{\partial}{\partial a_y})^m (-i \frac{\partial}{\partial a_z})^n J^{(0)} \quad (12)$$

where  $J^{(0)}$  is given by

$$J^{(0)} = \frac{2\pi}{\alpha} e^{-\alpha R_i^2 + \frac{A^2}{4\gamma}} M^{(0)}\left(\frac{1}{2}, \frac{3}{2}, \frac{-B^2}{4\gamma}\right) \quad (13)$$

and  $A^2 = -a^2 + 4\beta R_i^2 + 4i\beta\vec{a}\cdot\vec{R}_i$ ,  $B^2 = -a^2 + 4\alpha R_i^2 + 4i\alpha\vec{a}\cdot\vec{R}_i$ ,  $\gamma = \alpha + \beta$  and  $M^{(0)}$  is the confluent hypergeometric function of the first kind [25]. Using Eq.(12) and the notation  $M^{(k)}(a, b, z) = \frac{d^k}{dz^k} M(a, b, z)$  the following recursion relation is then obtained:

$$V_{lmn}^{(k)} = \frac{(l-1)}{2\gamma} V_{(l-2)mn}^{(k)} + \left(\frac{i}{2\gamma}\right)(v_x + 2i\beta R_x) V_{(l-1)mn}^{(k)} - \frac{(l-1)}{2\gamma} V_{(l-2)mn}^{(k+1)} + \left(\frac{i}{2\gamma}\right)(-v_x + 2i\alpha R_x) V_{(l-1)mn}^{(k+1)} \quad (14)$$

The relations are initiated by the direct evaluation of  $S_{lmn}$  and  $V_{lmn}^{(k=0)}$  for  $l, m, n = 0$  and 1 from Eq.(10) and Eq.(12), respectively. Equivalent relations for all terms are obtained by circular permutation of  $l, m$  and  $n$  in Eqs. (11) and (14).

### III. RESULTS AND DISCUSSION

#### A. Excitation to H(n=2) and H(n=3) states

We have computed the cross sections with several GTO basis sets, which are presented in Supplementary data. The exponents of the GTO have been chosen to follow modified geometric series. The largest and smallest values of the exponents in the basis set from B7 to B10 are set equal. However, the number of GTO included increases from B7 to B10 which provides a systematic procedure to improve the description of the atomic states and allow a careful convergence study. All basis sets include orbitals up to ( $n=6$  and  $\ell=5$ , i.e. 6h) for both target and projectile. Energy of the states in each basis set are compared to the exact ones in Supplementary data. Furthermore, the basis sets have a large number of pseudostates (states of positive energy obtained from the diagonalization of the isolated  $\text{Li}^{2+}$  and H Hamiltonian matrices expressed in the GTO basis sets) with energy up to 1 eV.

Cross sections obtained with the different basis sets are compared to previous results in Fig. 2 and 3 for excitation into H( $n=2$ ) and H( $n=3$ ), respectively. Cross sections for excitation into H( $n=2$ ) are nearly identical for all our basis sets which demonstrates the

convergence of the results. For excitation into  $H(n=3)$ , Fig. 3 shows that basis B7 is not sufficient to obtain converged cross sections within less than 10% uncertainties. However, the results obtained with B8, B9 and B10 do not differ significantly.

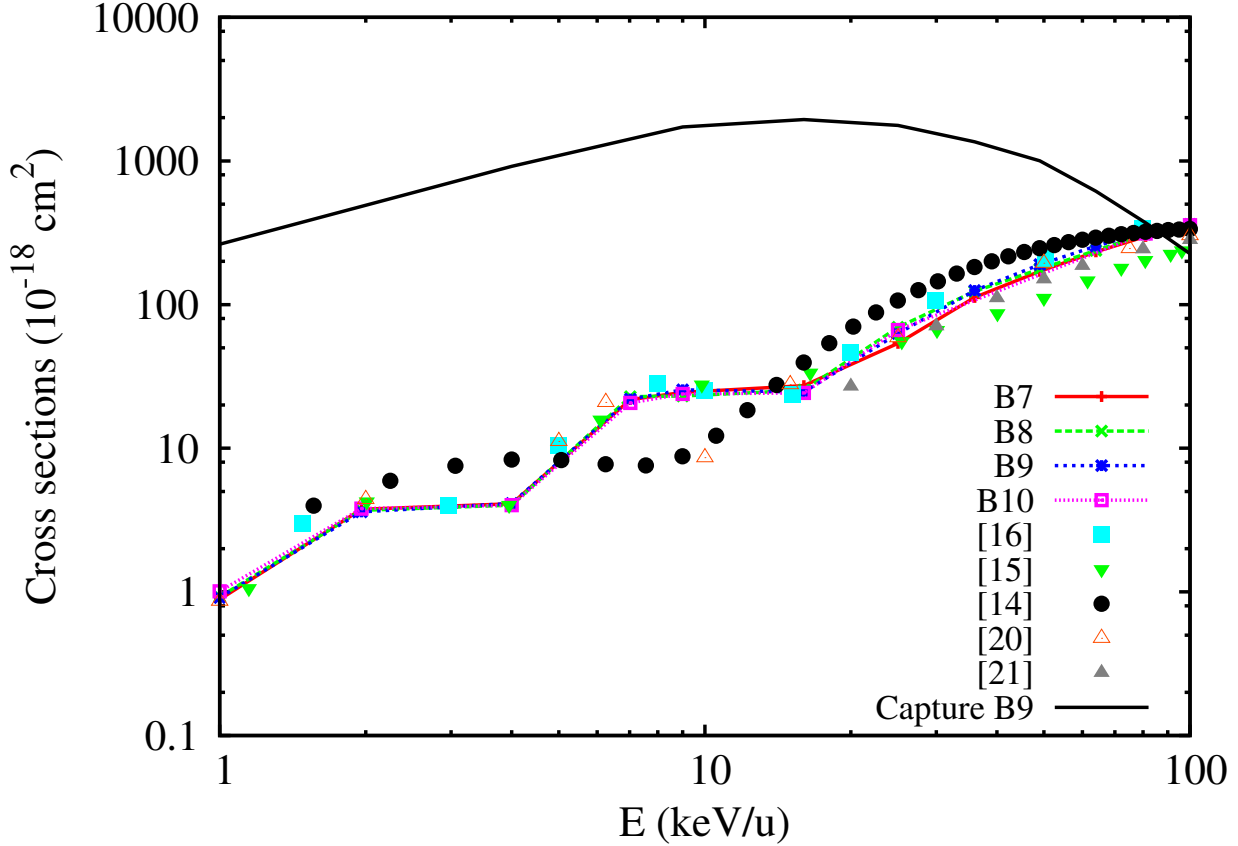


Figure 2. Cross sections for excitation into  $H(n=2)$  states.

The comparison with the previous results shows several important points. First, the analytical fits proposed by Murakani *et al.* [14] based on older data and scaling laws do not provide accurate cross sections for most of the impact energy range and for both excitation processes. Second, the cross sections obtained with previous close-coupling approaches [15, 16, 20] do not agree over the entire impact energy range. In particular, for energies above 30 keV/u the results from Liu *et al.*[16] are significantly larger than that from Suarez *et al.* [15]. Our results stand between these two sets of data for both excitation processes. Results from [16] and [15] are obtained with most recent close-coupling calculations. In [16], the authors use a two-center atomic orbital basis set in which hydrogen target states up to  $n=4$  and  $Li^{2+}$  projectile states up to  $n=6$  have been considered. No pseudo-states have

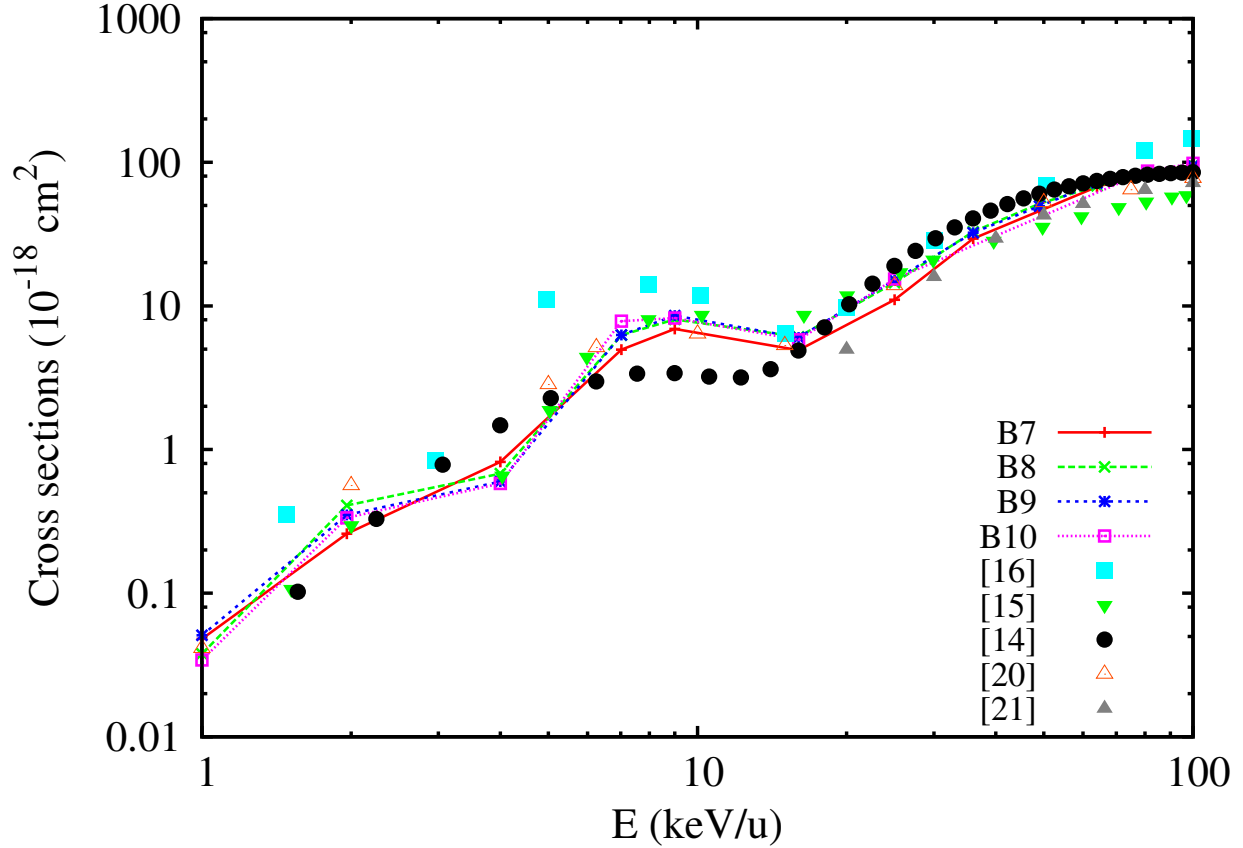


Figure 3. Cross sections for excitation into H( $n=3$ ) states. Same color code as in Fig.2.

been included in their calculations, so that ionization process is therefore neglected. In [15], the recommended cross sections are obtained from one-center close-coupling calculations for energy above 50-100 keV/u. In these calculations, the basis set is centered on the target nuclei. Ionization process is well described but capture processes, which may interfere with excitation processes in the energy range considered, are only taken into account via a finite numbers of pseudo-states. In order to illustrate the importance of the capture processes, the total cross sections computed with B9 are reported in Fig.2. The cross sections, which agree well with the results of Harel et al. [10], are larger than all excitation cross sections over the entire energy range, except for excitation into  $n=2$  at the highest collision energy (see for example [14] and references therein for further discussions on the capture cross-sections). The disagreements between the data from [16] and [15] come from neglecting one or the other process channel in their approaches. Our approach includes both processes and the corresponding results should be more accurate.

In order to demonstrate the importance of including both ionization and capture processes in the calculations, we have computed the cross sections with basis B9 but including during the dynamical part (Eq. (4)) either only  $H(n=1-4)$  and  $Li^{2+} (n=1-6)$  states as in [16] or only target states as in [15]. In the latter case, we have included pseudostates with energy up to 85 eV to approximately treat the ionization and capture flux as in [15]. Results for excitation into  $H(n=3)$ , for which the disagreements are the largest, are shown in Fig. 4.

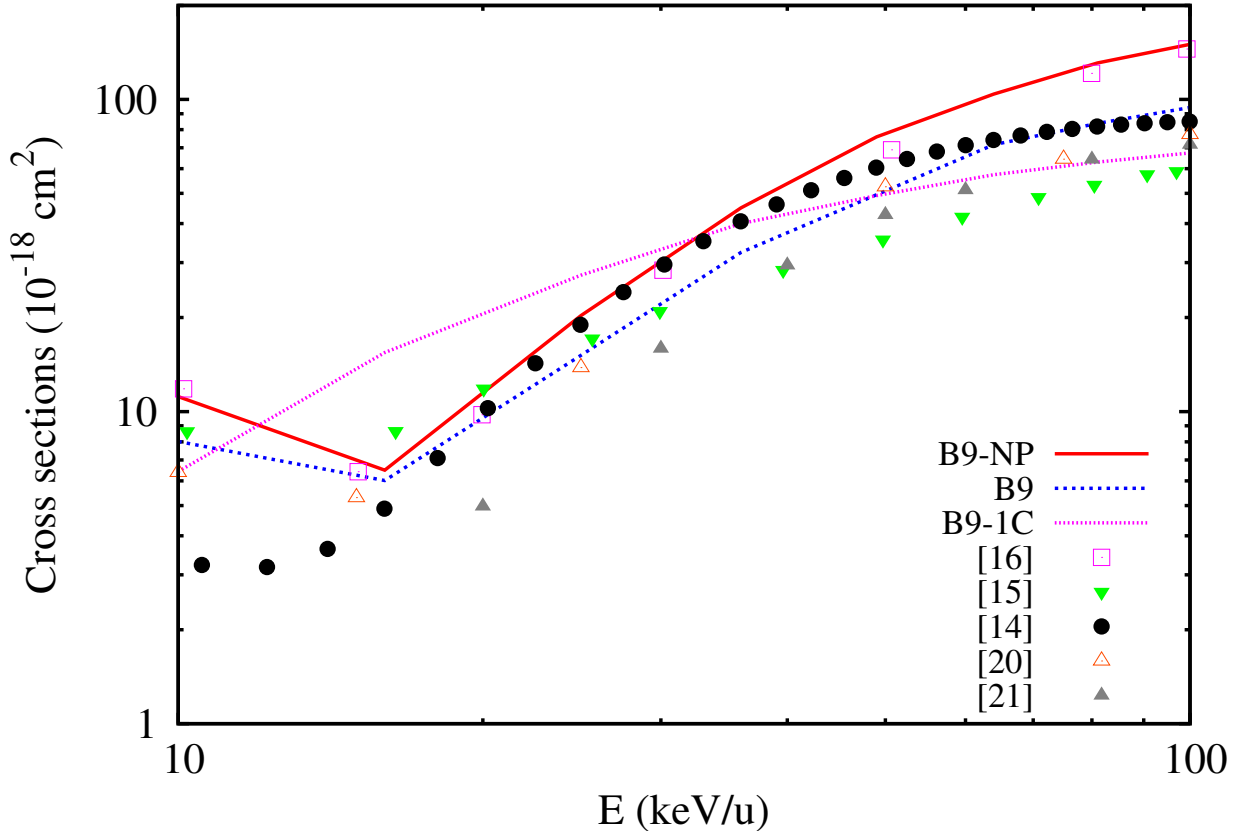


Figure 4. Cross sections for excitation into  $H(n=3)$  states obtained with limited basis sets. Results labelled B9-NP are obtained with the basis B9 without pseudostates (i.e. only  $H(n=1-4)$  and  $Li^{2+} (n=1-6)$  states are included). Results labelled B9-1C are obtained with the basis B9 for the target states and no projectile states (i.e. one-center expansion).

Cross sections obtained with the basis set B9 containing only  $H(n=1-4)$  and  $Li^{2+} (n=1-6)$  states (labeled B9-NP in Fig. 4) are larger than that obtained with the complete B9 set. These results are close to that of [16] since same channels are included in the calculations. However, it should be noted that the description of the atomic states are different. In [16],

they use Slater type orbitals while we use GTO, which shows that our choice of GTO is suitable to describe these states. Cross sections with only target states (B9-1C in Fig. 4) are smaller than that computed with the complete B9 set which seems to indicate that the one-center expansion of [15] is not appropriate at impact energy below 100 keV/u (it should be noted that the cross sections of [15] for energy below 50 keV/u are computed with different methods which treat well the capture channels). Same conclusions are reached for excitation into  $H(n=2)$  and  $H(n > 3)$  (not shown). Note that our one-center calculations do not reproduce completely the results of [15] but only the trends. Bessel functions are used in [15], so that while we expect to have a rather similar description of the bound target states, the ionization channels are better treated in [15], which explains the differences in cross sections. It should be mentioned that the differences between our cross sections and that reported by Toshima and Tawara [20] are difficult to discuss. In [20], the authors use the same method than us, i.e. two-center atomic orbital close-coupling with GTO. However, the GTO basis set they used is not completely defined in the paper which prohibits a direct comparison.

From the discussion above, we conclude that our cross sections for excitation into  $H(n=2)$  and  $H(n=3)$  states are the most accurate ones available to date. Based on these comparisons, we propose the cross sections into higher excited shells.

### **B. Excitation to $H(n=4-6)$ states**

Cross sections obtained with the different basis sets are compared to previous results in Fig. 5, 6 and 7 for excitation into  $H(n=4)$ ,  $H(n=5)$  and  $H(n=6)$ , respectively. For excitation into  $H(n=4)$ , our cross sections are well converged for energy above 30 keV/u. At lower impact energy, only B9 and B10 provide converged results for energy around 10 keV/u. At the lowest collision energy (1 keV/u), our results are not converged: the cross sections obtained with B9 and B10 differ by about a factor of 2.

For excitation into  $H(n=5)$  and  $H(n=6)$  states, the convergence with respect to basis set is not completely achieved. For excitation into  $H(n=5)$ , the cross sections obtained with the largest basis sets may differ by up to 20% while for excitation into  $H(n=6)$ , the 3 different data shown vary by less than 40%. The larger uncertainties on the cross sections for these channels may come from either a poorer description of the atomic states with GTO

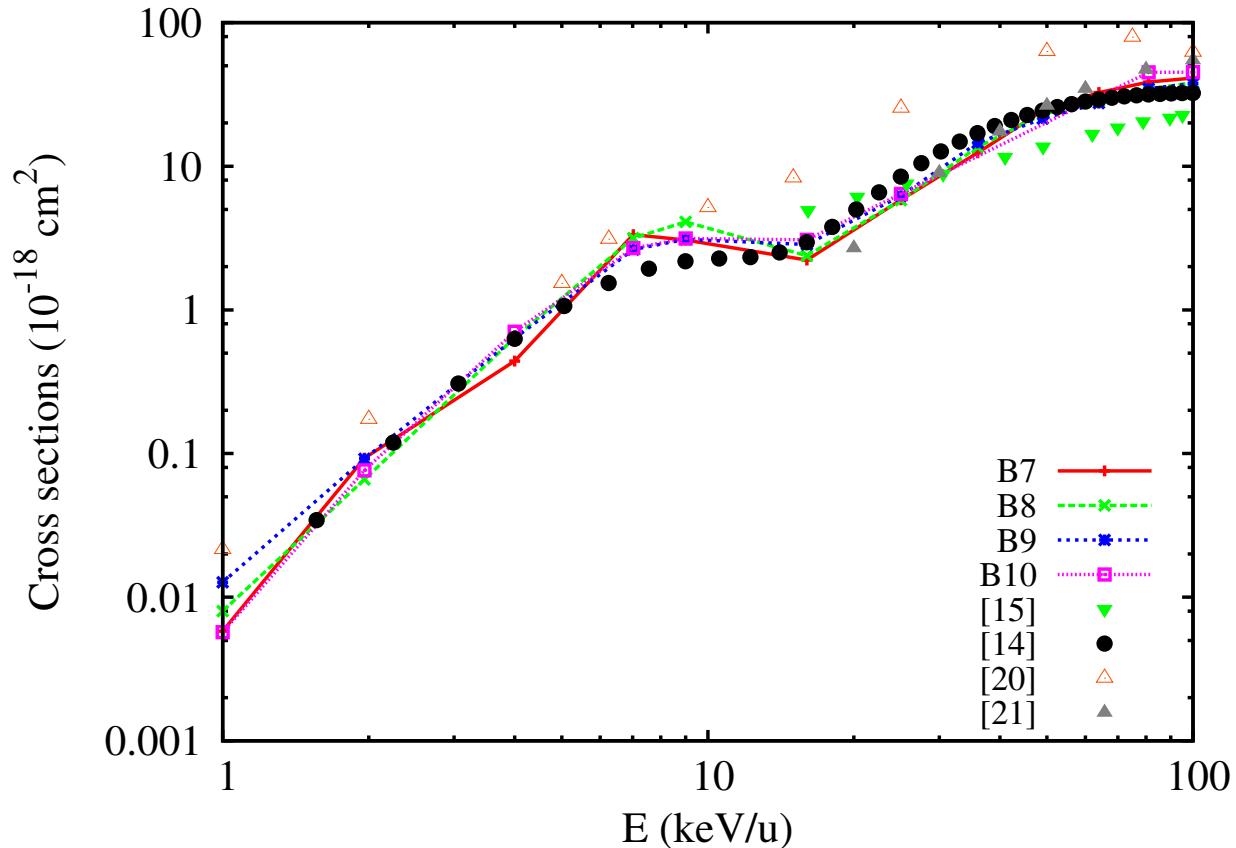


Figure 5. Cross sections for excitation into H( $n=4$ ) states. Same color code as in Fig.2.

compared to lowest atomic states or by stronger coupling with ionization and/or higher capture channels. At low collision energies for which the capture process is largely dominant, these excitation channels may be significantly coupled to capture pathways towards highly excited states of  $\text{Li}^{2+}$  (for example  $\text{Li}^{3+}\text{-H}(n=6)$  is asymptotically degenerated with  $\text{Li}^{2+}(n=18)\text{-H}^+$ ). At higher collision energies, ionization becomes significant and may be coupled to these excitation channels. Both effects are only approximately taken into account in our calculations with the use of the pseudo-states. Including more GTO for each angular momentum and adding higher angular momentum ones would improve the convergence of the results. However, the cost in CPU time for larger basis sets limits such calculations in the present time. It should however be noted that even with the uncertainties of our cross sections it is seen that the cross sections recommended in [14] and [15] are not accurate. In [14], the authors use scaling laws that do not seem to be valid. The lower cross sections obtained in [15] come from their one-center expansion as discussed in the previous section.

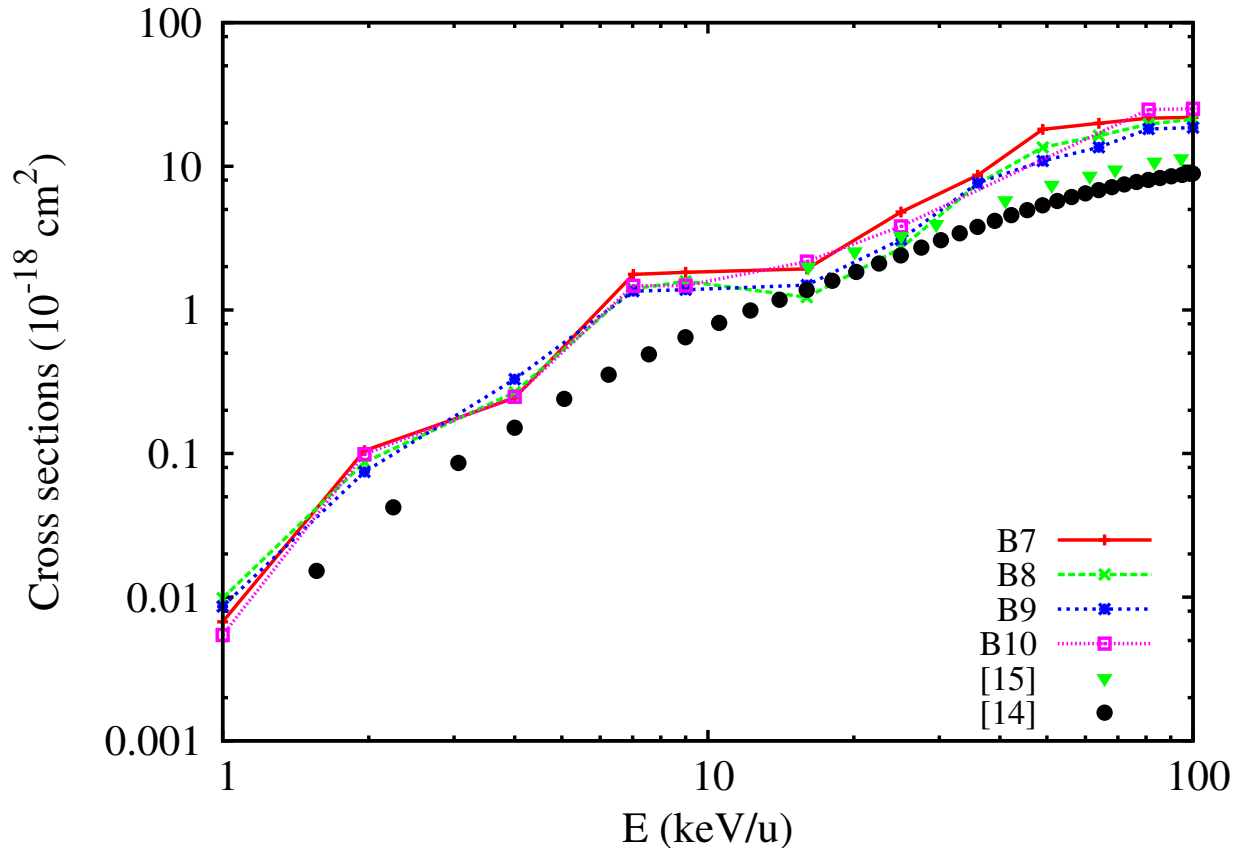


Figure 6. Cross sections for excitation into  $H(n=5)$  states. Same color code as in Fig.2.

### C. State-selective cross sections

The state-selective cross sections computed with the basis sets B8 and B9 are given in tables I, II, III, IV and V. At the highest collision energies considered here and for low excited states of atomic hydrogen, the dipole allowed transitions ( $1s \rightarrow np$ ) are the dominant ones. This has been discussed in [12] and references therein: at collisions energies above 50 keV/u and for excitation into  $H(n=2)$  and  $H(n=3)$  states the excitation process takes place at large impact parameters (larger than 5 a.u. in the present case), i.e. large distances between the projectile and target centers, in which the dipole term in the multipole expansion of projectile-target interaction is dominant. At lower impact energies and for higher excited states, the excitation process is effective at smaller impact parameters such that higher-order terms of the expansion contribute substantially.

The results of [12], [20] and [21] (up to  $H(4f)$ ) are also reported for comparison. The relative difference between the results of the two basis sets may be used as uncertainties

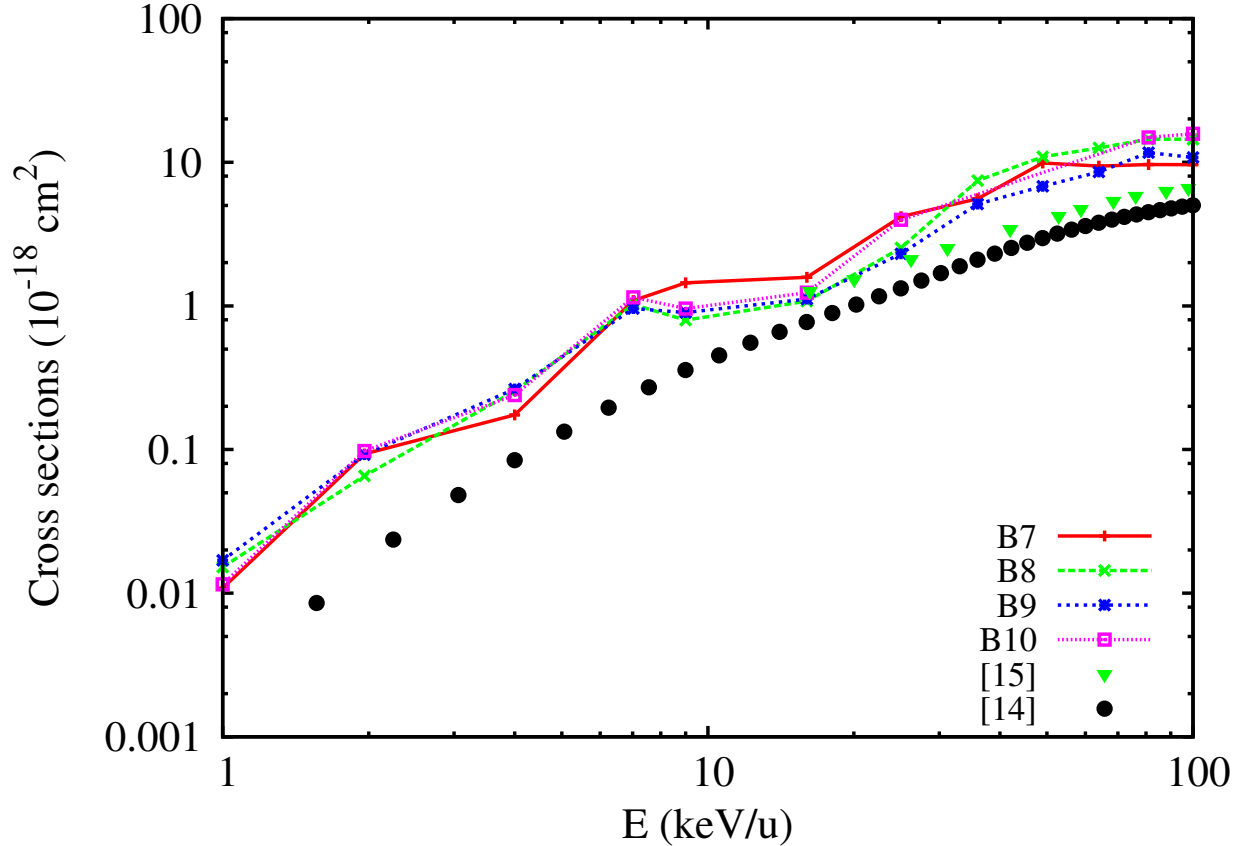


Figure 7. Cross sections for excitation into H( $n=6$ ) states. Same color code as in Fig.2.

of the cross sections obtained with B9, which are the most accurate ones in the present work. For cross sections smaller than  $10^{-18} \text{cm}^2$  and for excitation into high-lying states, the uncertainties may be quite large: between 20 to 70% in general, and reaching up to 200% in few values. For the other cross sections, the uncertainties are below 15%. It should be mentioned that our results differ, sometimes substantially, to the results of [20] and [21]. Owing to the discussion on the  $n$ -resolved cross sections, we believe the values given in the present work are more accurate.

#### IV. CONCLUSION

In conclusion we have presented a new implementation of the two-center atomic orbital close-coupling approach for describing electronic processes in collisions between multiply charged ions and single-active electron target systems. This approach has been applied to  $\text{Li}^{3+}$  - H collisions in the 1-100 keV/u impact energy range. In the present work, we have

reported the cross sections for excitation into high-lying states for which large discrepancies between previous works were observed. Our extensive calculations and a careful convergence study have permitted to understand the differences between the previously obtained cross sections and have provided accurate ones for excitation up to H(n=6).

## V. ACKNOWLEDGEMENTS

This work has been financially supported by the ANR within the Investissements d’Avenir programme under reference ANR-11-IDEX-0004-02 (Labex Plas@par).

- 
- [1] Anderson H, von Hellermann M G, Hoekstra R, Horton L D, Howman A C, Konig R W T, Martin R, Olson R E and Summers H P 2000 *Plasma Phys. Control. Fusion* **42** 781
  - [2] M. G. von Hellermann *et al.* 2005 *Phys. Scr.* **120** 19
  - [3] E. Delabie *et al.* 2010 *Plasma Phys. Control. Fusion* **52** 125008
  - [4] Abrines R and Perceval I C 1966 *Proc. Phys. Soc.* **88** 861
  - [5] Maruhn-Rezwani W 1979 *Phys. Rev. Lett.* **43** 512
  - [6] Olson R E 1981 *Phys. Rev. A* **24** 1726
  - [7] Janev R K, Belic D S and Brandsen B H 1983 *Phys. Rev. A* **28** 1293
  - [8] Fritsch W and Lin C D 1984 *Phys. Rev. A* **29** 3039
  - [9] Gilbody H B 1989 *Phys. Scripta* **T28**
  - [10] Harel C, Jouin H and Pons B 1998 *At. Dat. and Nucl. Dat. Tab.* **68** 279
  - [11] Kolakowska W, Pindzola M S and Schultz D R 1999 *Phys. Rev. A* **59** 3588
  - [12] Martin F 1999 *J. Phys. B: At. Mol. Opt. Phys.* **32** 501
  - [13] Caillat J, Dubois A and Hansen J P 2000 *J. Phys. B: At. Mol. Opt. Phys.* **33** L715
  - [14] Murakami I, Yan J, Sato H, Kimura M, Janev RK, Kato T 2008 *At. Dat. and Nucl. Dat. Tab.* **94** 161
  - [15] Suarez J, Guzman F, Pons B and Errea L F 2013 *J. Phys. B: At. Mol. Opt. Phys.* **46** 095701
  - [16] Liu L, Li X Y, Wang J G and Janev R K 2014 *Physics of Plasmas* **21** 062513
  - [17] Gu M F, Holcomb C T, Jayakuma R J and Allen S L 2008 *J. Phys. B: At. Mol. Opt. Phys.* **41** 095701

- [18] Iwamae A, Sakaue A, Atake M, Sawada K, Goto M and Morita S 2009 *Plasma Phys. Control. Fusion* **51** 115004
- [19] Ralchenko Y, Marchuk O, Biel W, Schlummer T, Schultz D R and Stambulchik E 2012 *Rev. Sci. Instrum.* **83** 10D504
- [20] Toshima N and Tawara H 1995 *National Institute for Fusion Science Report NIFS-DATA-26*
- [21] Purkait M 2008 *Nucl. Instrum. Methods Phys. Res. B* **266** 1957
- [22] Fritsch W and Lin C D 1991 *Phys. Rep.* **202** 1
- [23] *Charge Exchange and the Theory of Ion-Atom Collisions*, B.H. Bransden et M.R.C McDowell, Oxford University Press, 1992.
- [24] Cherkes I, Klaiman S and Moiseyev N 2009 *Int. J. of Quant. Chem.* **109** 2996
- [25] Abramowitz M and Stegun I A 1964 *Handbook of Mathematical Functions, National Bureau of Standards Applied Mathematics Series* **55**

E(keV/u)	2s					2p				
	B8	B9	T	P	M	B8	B9	T	P	M
1.0	0.331	0.308	0.329	-	-	0.591	0.604	0.533	-	-
4.0	1.046	1.054	3.87	-	-	2.971	3.077	7.29	-	-
9.0	5.521	6.023	6.31	-	-	17.57	19.46	2.28	-	-
16.0	11.63	12.53	10.6	-	-	13.74	12.07	17.1	-	-
25.0	32.60	28.55	22.7	-	-	36.98	34.37	36.2	-	-
36.0	47.96	47.29	36.0	-	-	75.71	77.90	70.4	-	-
49.0	41.42	41.30	62.9	23.0	-	135.0	148.4	131.0	127.0	-
64.0	36.30	39.17	-	-	-	201.7	216.4	-	-	-
81.0	42.59	43.13	-	-	50.1	266.0	278.0	-	-	214.8
100.0	48.70	51.88	54.6	29.4	43.7	309.4	310.0	248.0	253.0	232.5

Table I. State-selective excitation cross sections computed with basis sets B8 and B9 (in  $10^{-18} \text{cm}^2$ ). Results are compared to that of Martin [12] (labeled M), Toshima et al. [20] (labeled T) and Purkait [21] (labeled P). Values for T at E=4.0, 9.0, 16.0 and 49.0 keV/u are that of E=5.0, 10.0, 15.0 and 50.0 keV/u from [20], respectively.

E(keV/u)	3s					3p					3d				
	B8	B9	T	P	M	B8	B9	T	P	M	B8	B9	T	P	M
1.0	0.009	0.016	0.012	-	-	0.017	0.016	0.0168	-	-	0.010	0.018	0.0125	-	-
4.0	0.097	0.140	0.458	-	-	0.266	0.164	0.897	-	-	0.316	0.293	1.48	-	-
9.0	1.472	1.304	0.744	-	-	4.096	4.253	3.53	-	-	2.483	2.987	2.11	-	-
16.0	1.483	1.507	1.93	-	-	2.646	2.496	1.82	-	-	1.956	2.007	1.55	-	-
25.0	4.975	4.290	3.94	-	-	4.800	5.170	6.31	-	-	4.724	5.687	3.58	-	-
36.0	13.06	12.96	10.5	-	-	8.562	9.340	15.6	-	-	11.21	10.02	5.84	-	-
49.0	14.25	12.50	13.2	9.0	-	15.73	18.88	26.9	24.0	-	21.39	18.09	12.4	9.6	-
64.0	9.294	9.831	-	-	-	29.73	31.29	-	-	-	29.46	30.53	-	-	-
81.0	8.257	9.190	-	-	10.1	41.18	40.78	-	-	36.9	33.89	33.81	-	-	13.2
100.0	9.711	9.336	13.0	10.0	8.9	51.43	51.51	47.5	46.5	39.6	33.54	33.34	16.7	15.1	13.3

Table II. State-selective excitation cross sections computed with basis sets B8 and B9 (in  $10^{-18} \text{cm}^2$ ). Same notation as in Tab. I is used.

E(keV/u)	4s						4p						4d						4f					
	B8	B9	T	P	M		B8	B9	T	P	M		B8	B9	T	P	M		B8	B9	T	P	M	
1.0	0.000	0.001	0.003	-	-		0.004	0.003	0.001	-	-		0.002	0.003	0.012	-	-		0.001	0.003	0.002	-	-	
4.0	0.057	0.068	0.29	-	-		0.206	0.250	0.383	-	-		0.236	0.179	0.31	-	-		0.140	0.135	0.549	-	-	
9.0	1.175	0.540	0.777	-	-		0.457	0.717	1.79	-	-		0.908	0.830	1.54	-	-		1.554	1.014	1.05	-	-	
16.0	0.545	0.405	2.23	-	-		1.120	1.116	3.5	-	-		0.445	0.636	1.92	-	-		271	0.696	0.659	-	-	
25.0	1.199	1.250	7.47	-	-		1.723	2.213	10.8	-	-		1.700	1.833	5.83	-	-		1.193	0.923	1.29	-	-	
36.0	4.461	4.515	14.9	-	-		3.096	3.799	23.0	-	-		4.167	4.445	11.7	-	-		1.853	1.811	1.43	-	-	
49.0	5.601	4.825	17.6	1.8	-		6.041	5.970	28.4	11.3	-		8.428	7.162	14.7	9.8	-		3.012	3.511	2.3	3.4	-	
64.0	3.434	3.173	-	-	-		10.38	9.701	-	-	-		10.75	11.16	-	-	-		3.804	3.514	-	-	-	
81.0	2.847	3.180	-	-	3.6		14.34	14.16	-	-	12.5		13.33	14.31	-	-	5.7		3.878	3.031	-	-	1.2	
100.0	3.327	3.116	13.1	2.2	3.2		18.13	17.22	30.7	24.8	14.1		13.23	14.60	15.6	20.5	5.8		3.557	2.660	2.91	7.2	0.97	

Table III. State-selective excitation cross sections computed with basis sets B8 and B9 (in  $10^{-18} \text{cm}^2$ ). Same notation as in Tab. I is used.

E(keV/u)	5s		5p		5d		5f		5g	
	B8	B9								
1.0	0.000	0.000	0.001	0.002	0.003	0.002	0.002	0.001	0.002	0.002
4.0	0.024	0.018	0.048	0.043	0.045	0.016	0.059	0.074	0.087	0.175
9.0	0.443	0.233	0.212	0.254	0.343	0.373	0.188	0.227	0.396	0.292
16.0	0.170	0.209	0.478	0.556	0.198	0.282	0.224	0.317	0.153	0.121
25.0	0.350	0.566	0.712	1.196	0.722	0.709	0.724	0.432	0.182	0.186
36.0	1.892	1.868	1.549	1.890	2.408	1.923	1.481	1.332	0.223	0.630
49.0	2.760	2.167	3.553	2.743	4.792	3.518	2.111	2.203	0.302	0.268
64.0	1.863	1.438	5.771	4.630	5.672	5.145	2.814	2.196	0.176	0.154
81.0	1.552	1.519	7.889	7.118	7.333	7.209	2.728	2.228	0.141	0.079
100.0	1.763	1.363	9.677	7.824	7.016	7.408	2.689	1.891	0.112	0.093

Table IV. State-selective excitation cross sections computed with basis sets B8 and B9 (in  $10^{-18}cm^2$ ).

E(keV/u)	6s		6p		6d		6f		6g		6h	
	B8	B9										
1.0	0.000	0.000	0.000	0.001	0.006	0.003	0.004	0.002	0.001	0.004	0.001	0.003
4.0	0.007	0.025	0.033	0.024	0.041	0.026	0.065	0.066	0.025	0.030	0.082	0.089
9.0	0.123	0.109	0.080	0.135	0.223	0.228	0.074	0.159	0.193	0.198	0.102	0.067
16.0	0.055	0.142	0.164	0.330	0.258	0.218	0.410	0.242	0.158	0.170	0.032	0.011
25.0	0.164	0.395	0.615	0.873	0.836	0.505	0.731	0.361	0.172	0.143	0.015	0.026
36.0	1.261	1.076	1.816	1.112	2.521	1.194	1.479	1.154	0.346	0.546	0.033	0.026
49.0	1.851	1.154	3.194	1.601	3.742	2.120	1.825	1.612	0.285	0.296	0.023	0.020
64.0	1.415	0.790	4.912	2.951	3.924	3.033	2.174	1.617	0.144	0.145	0.015	0.010
81.0	1.212	0.828	6.112	4.480	5.030	4.492	1.986	1.764	0.127	0.091	0.010	0.012
100.0	1.218	0.676	6.893	4.270	4.345	4.427	1.892	1.313	0.099	0.117	0.009	0.005

Table V. State-selective excitation cross sections computed with basis sets B8 and B9 (in  $10^{-18}cm^2$ ).